DESY 94-231

On the Kinematic Reconstruction of Deep Inelastic Scattering at HERA: the Σ Method

Ursula Bassler, Gregorio Bernardi

Laboratoire de Physique Nucléaire et de Hautes Energies
Université de Paris VI-VII, 4 Place Jussieu, Paris 75230 cedex 05, France

Abstract

We review and compare the reconstruction methods of the inclusive deep inelastic scattering variables used at HERA. We introduce a new prescription, the Sigma (Σ) method, which allows to measure the structure function of the proton $F_2(x, Q^2)$ in a large kinematic domain, and in particular in the low x-low Q^2 region, with small systematic errors and small radiative corrections. A detailed comparison between the Σ method and the other methods is shown. Extensions of the Σ method are presented. The effect of QED radiation on the kinematic reconstruction and on the structure function measurement is discussed.

1 Introduction

The measurement of the structure functions of the nucleon requires a precise reconstruction of the deep inelastic scattering (DIS) kinematics. With the advent of HERA, the first electron-proton collider ever built, this reconstruction needs not anymore to rely on the scattered lepton only, since the most important part of the hadronic system is visible in the 4π detectors H1 and ZEUS. This redundancy allows for an experimental control of the systematic errors on the structure function measurement if it is based on several independent methods to determine the usual DIS kinematic variables x, y and Q^2:

$$x = \frac{Q^2}{2P.q} \qquad\qquad y = \frac{P.q}{P.k} \tag{1}$$

$$Q^2 = -(k-k')^2 = -q^2 \qquad\qquad Q^2 = xys \tag{2}$$

with s being the center of mass energy squared, P, k the 4-vectors of the incident proton and lepton and k' the scattered lepton one. In this report we briefly review in section 2 the methods used at HERA in the first year of operation. We introduce in section 3 a new way to compute the kinematics, the Σ method, which allows a precise F_2 measurement in the complete kinematical region accessible at HERA including the low x-low Q^2 region. We then make two rather detailed comparisons of the Σ, the mixed, the double-angle and the electron methods at low x and at high Q^2 (sect.4). Extensions of the Σ method, including a prescription for kinematic fitting are given in section 5. We examine the effect of QED radiation on the F_2 measurement (sect.6). Two methods independent of initial state QED radiation are defined and compared in section 7. The main conclusions are summarized in section 8.

2 Kinematic Reconstruction Methods at HERA

In the naive quark-parton model, the lepton scatters elastically against a quark of the proton, and the two body final state is completely constrained using two variables, if we know the initial energies labeled E^e and E^p for the electron and proton. Denoting E, θ and F_q, γ_q the energy and angle of the electron and of the struck quark (which gives rise to the "current jet"), we can derive y and Q^2 by combining any 2 of them. For a scattered quark F_q and γ_q are well defined observables, but what is actually observed after a collision is a set of particles making energy deposition in the detector. After identification of the scattered electron, we can define 2 independent quantities: Σ, defined as the sum of the scalar quantities $E_h - p_{z,h}$ of each particle belonging to the hadronic final state, and T as its total transverse momentum.

$$\Sigma = \sum_h (E_h - p_{z,h}) \qquad\qquad T = \sqrt{(\sum_h p_{x,h})^2 + (\sum_h p_{y,h})^2} \tag{3}$$

$E_h, p_{x,h}, p_{y,h}, p_{z,h}$ are the four-momentum vector components of each hadronic final state particle. From energy-momentum conservation we can then define an inclusive angle γ but also an inclusive energy F of the hadronic final state which would be the same as the angle and energy of the scattered quark in the naive quark-parton model. The formulae which allow to go from Σ, T to F, γ are:

$$\tan\frac{\gamma}{2} = \frac{\Sigma}{T} \qquad\qquad F = \frac{\Sigma^2 + T^2}{2\Sigma} \tag{4}$$

Σ is by construction minimally affected by the losses in the forward direction[1] ($= 2E_i \sin^2 \frac{\theta_i}{2}$ for every lossed particle i) due to the beam pipe hole in which the target jet and the initial state gluon radiation tend to disappear. T covers the other spatial dimensions, but it is more sensitive to forward losses ($= E_i \sin\theta_i$), thus to improve kinematic reconstruction we should try to avoid using it. We can use γ instead, which carries the T information and is better measured since in the ratio Σ/T the energy uncertainties cancel and the effect of the losses in the forward beam pipe is diminished. In conclusion the optimal four "detector oriented" variables to characterize deep inelastic scattering at HERA are $[E, \theta, \Sigma, \gamma]$.

If we want to determine x and Q^2 from 2 variables out of these 4, we are left with 6 combinations of which only 3 have been shown to be usable for structure function measurement (the formulae are given in the appendix):

- the electron-only (e) method which uses E and θ is experimentally simple and very precise in the high y (> 0.2) region. It nevertheless degrades rapidly with decreasing y [1] due to the $1/y$ term in the error propagation[2] of y_e:

$$\frac{\delta y}{y} = \frac{1-y}{y} \left(\frac{\delta E}{E} \oplus \frac{\delta\theta}{\tan\theta/2}\right) \tag{5}$$

- the hadrons-only (h) method [2] provides a rather precise measurement of y at low and medium y ($y < 0.2$), which degrades at high y. It gives a rather poor measurement of Q^2 due to the loss of hadrons in the beam pipe but it is the only possible method for "charged current" events.

- the double-angle (DA) method [3, 4] uses the angle of the electron θ and the inclusive angle of the hadronic final state γ. Assuming an homogeneous energy measurement over the full solid angle, we can deduce from eq.4 that the DA method is independent of the absolute energy calibration. This method is precise at high Q^2 ($Q^2 > 100 GeV^2$) but has large resolutions at low x-low Q^2 [5], as will also be illustrated in section 4.

At HERA a fourth method has been used which combines y measured from the hadrons and Q^2 from the electron, which is the so-called mixed (m) method [6]:

$$x_m = \frac{Q^2_e}{s\ y_h} \qquad \text{with} \qquad y_h = \frac{\Sigma}{2E^e} \tag{6}$$

The mixed method allows to extend towards lower y the F_2 measurement done with the DA method [5] or with the e method [5, 7]. Note that in the mixed method more than 2 independent variables are used, i.e. E, θ and Σ, justly avoiding T, and we will see in the next section that these 3 variables can be combined in a more efficient way. The basic methods presented above become imprecise in some places of the kinematic domain. To have a single method covering the complete kinematic region measurable at HERA we can either make use of the kinematic fitting procedure (see sect.5) or explore further combinations of the 4 variables $[E, \theta, \Sigma, \gamma]$ (sect.3 and 7).

[1] The positive z axis is defined at HERA as the incident proton beam direction. The electron polar angle is thus large ($\sim 170^o$) for small scattering angle, i.e. small Q^2.

[2] We define $A \oplus B \equiv \sqrt{A^2 + B^2}$

3 The Σ method

With 3 variables, we can determine y and Q^2 independently of initial state QED radiation (ISR) by reconstructing the incident electron energy. From energy-momentum conservation, the measured quantity Δ is equal to two times the electron beam energy, if no particle escape detection:

$$\Delta \equiv \Sigma + E(1-\cos\theta) = 2E^e \tag{7}$$

We can then obtain from y_h a new expression y_Σ [8] which gives y at the hard interaction vertex even if an ISR photon is emitted.

$$y_\Sigma = \frac{\Sigma}{\Sigma + E(1-\cos\theta)} \tag{8}$$

y_Σ has another important characteristic: at high y, i.e in the most interesting region at low Q^2, Σ dominates over $E(1-\cos\theta)$, and the fluctuations and errors on Σ start cancelling between numerator and denominator, allowing an optimal y reconstruction when using the hadrons. Writing the error propagation on y_Σ,

$$\frac{\delta y}{y} = (1-y)\,(\frac{\delta\Sigma}{\Sigma} \oplus \frac{\delta E}{E} \oplus \frac{\delta\theta}{\tan\theta/2}) \tag{9}$$

we can observe the following differences with y_e (eq.5) and y_h ($\delta y_h/y_h = \delta\Sigma/\Sigma$):
i) At low y there is no divergence of $\delta y/y$ for y_Σ, which has practically the same behaviour as y_h since the $\delta\Sigma/\Sigma$ term is experimentally bigger than the two terms coming from the electron measurement.
ii) at high y, the error on y decreases as $(1-y)$ for y_Σ but is still dominated experimentally by the error on Σ. The $\delta\Sigma/\Sigma$ term is partly compensated by the $(1-y)$ term contrarily to the y_h case.

In fig.1 is shown the behaviour at low x-low Q^2 (see sect.4.1 for the description of the sample of Monte Carlo events used here) of the correlation y_Σ/y_e compared to y_h/y_e and to y_{DA}/y_e. These predicted behaviours have been reproduced by the H1 collaboration for the F_2 analysis on the 1993 data [9]. We can observe the expected improvement of y_Σ at high y, despite the worsening of y_h due to the low energy of the hadronic final state[3]. In this plot $y = 0.5$ corresponds in average to $x \sim 2.10^{-4}$.

From E, θ and Σ we determine Q^2_Σ, also independent of ISR when assuming that an initial state radiated photon which is colinear to the beam line do not carry transverse momentum.

$$Q^2_\Sigma = \frac{E^2\sin^2\theta}{1-y_\Sigma} \tag{10}$$

From $Q^2 = xys$ we can obtain x_Σ in two ways:
i) taking the "true" s at the hard interaction vertex, as will be dicussed in section 7. ii) taking s as computed from the beam energies ($s = 4E^eE^P$):

$$x_\Sigma = \frac{Q^2_\Sigma}{sy_\Sigma} = \frac{E^2\sin^2\theta}{s\ y_\Sigma(1-y_\Sigma)} \tag{11}$$

[3]This effect is amplified in the H1 detector by the poor hadronic calorimeter coverage in the backward direction, in which the hadronic final state particles tend to go at high y. We can remark that y_Σ is relatively insensitive to this peculiarity.

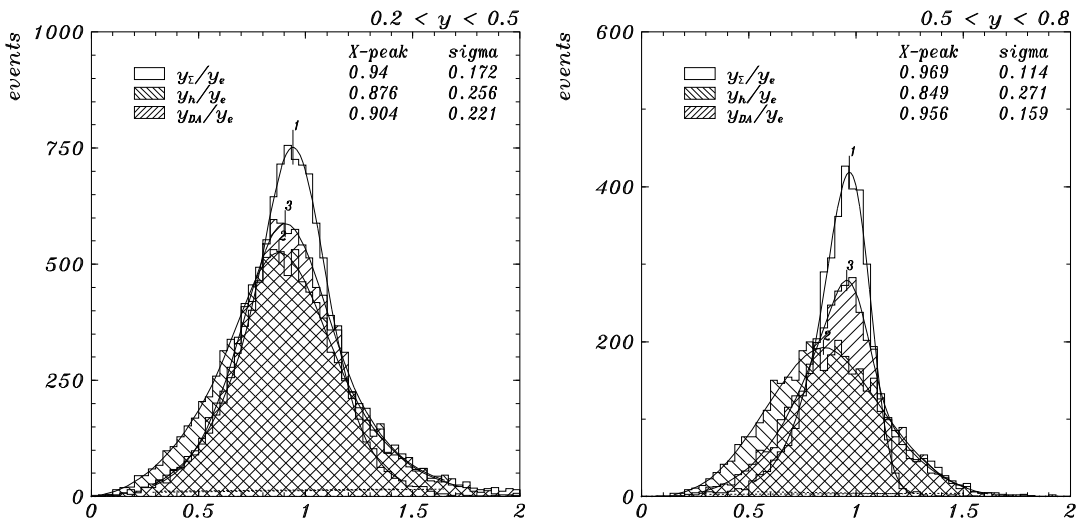

Figure 1: *Monte Carlo comparison of y reconstruction for several hadronic methods w.r.t. to y_e, at high (0.2-0.5) and very high y (0.5-0.8). Both bias and resolution improve with y for the Σ method although these become worse for the hadrons-only method. y_{DA} has larger biases and resolutions than y_Σ, as can be read from the fit results written inside the figure.*

Thus we have defined a new method, which has similar characteristics as the mixed method at low and medium y, but a higher precision at high y allowing to cross-check the e method in this region. It must be stressed that this improvement does not come from the precision of the electron measurement, on which on the contrary relies the precision of the e method. These methods then provide two measurements essentially independent. Finally y_Σ and Q^2_Σ being ISR independent, the radiative corrections to the Σ method are smaller than to the other methods (see sect.6).

4 Comparison of Electron, DA, Mixed and Σ methods

We study in this section the resolutions and biases of the x and Q^2 variables as reconstructed by the different methods. The Monte Carlo event sample on which this study is based has been generated according to cross-section above 5 GeV^2, with the DJANGO [10] program which relies on HERACLES [11] for the treatment of QED radiation, and for the simulation of the hadronic final state on the color dipole model (CDM) as implemented in ARIADNE [12]. The CDM is known to give the best description of the energy flow on the HERA data [13, 14]. The MRSH [15] parton densities parametrizations, which include the constraints from the 1992 HERA data were used. The generated events were then processed through the H1 analysis chain, which includes a detailed simulation based on GEANT [16] of the H1 detector [17]. Thus the results presented here after include in a realistic way the effect of inhomogeneities or small miscalibrations encountered in a real detector. The conclusions that we will draw are nevertheless general, since the characteristics of the H1 and ZEUS detectors are rather similar after the major detector effects are corrected by the reconstruction program. To make a meaningful comparison, all methods are applied on the same events using the same H1KINE [18] software package which is part of the H1 reconstruction program. One of its characteristics is to use a combination of track momentum and calorimetric energy in the

central part of the detector ($25^o < \theta < 155^o$) to improve the precision on the hadronic final state measurement and in particular to render it sensitive to the low energy hadrons ($E_h < 0.5\ GeV$) present in large number at low Q^2. This treatment is applied consistently to all reconstruction methods.

The structure function analysis is generally done in bins of x and Q^2, thus we will study here the following distributions[4]: x_{method}/x and Q^2_{method}/Q^2. No bias on the reconstructed variable is observed when the distribution peaks at 1. In order to conserve a good proportion of events originating from a given bin in that bin (defined as the "purity" of the bin) we need to have small biases and good resolutions on x and Q^2. The better the resolution the finer binning we can reach, assuming we have enough events, and thus the more subtle effects in the F_2 evolution along x or Q^2 can be observed. This is particularly true at low x where the number of events collected in the first three years of operation is large enough to make the finest binning allowed by the detector resolutions.

We will focus successively on two very different kinematic regions, for obvious physical reasons: the low x domain ($x < 10^{-3}$) which at HERA is accessible only below $\sim 50\ GeV^2$, and the high Q^2 domain which we will define as $Q^2 > 200\ GeV^2$. In both cases, the events must also satisfy the following conditions: $\theta < 173^o$, $E > 8\ GeV$, $\Delta > 30\ GeV$, this last condition being helpful to reduce radiative effects and, on data, the background to the deep inelastic interactions. However for the distributions shown in the next two sections, only events without emitted photons from the electron line are used, in order not to mix the smearing due to the reconstruction method with the one coming from the radiation effect.

4.1 Comparison at Low x

For this study we ask: $Q^2 > 7\ GeV^2$. The results are shown in figs.2 and 3 for x and Q^2 respectively, with one column per method and 5 bins in y. We distinguish very high (0.5-0.8), high (0.2-0.5), medium (0.1-0.2), low (0.05-0.1) and very low y (0.01-0.05), reminding that the lowest x are at highest y and viceversa. From these distributions we can draw the following conclusions which are valid in the low Q^2 region:

- The Σ method has, as expected, a much more precise x reconstruction than the mixed method at high and very high y. The behaviour of x_Σ and x_m is almost identical at low and medium y.
- x_Σ is the only x which is reconstructed with small biases ($< 10\%$) and precise resolutions ($< 20\%$) over the full y range (0.01-0.8). x_{DA} can compete at low and medium y, but becomes very imprecise when y rises. x_e is slightly more precise than x_Σ at high y, then rapidly becomes imprecise with decreasing y.
- Q^2_e has always very small biases and optimal resolutions ($\sim 4\%$). Q^2_Σ has no bias and good resolution ($\sim 7\%$) at low and medium y, but becomes more imprecise with increasing y. Q^2_{DA} has the same tendency, but in a more extreme way: better resolution at low y ($\sim 3\%$) and poorer resolution at very high y.

[4]When x, y or Q^2 have not the subscript which corresponds to a given method, they are assumed to be the true i.e. generated values at the hard interaction vertex.

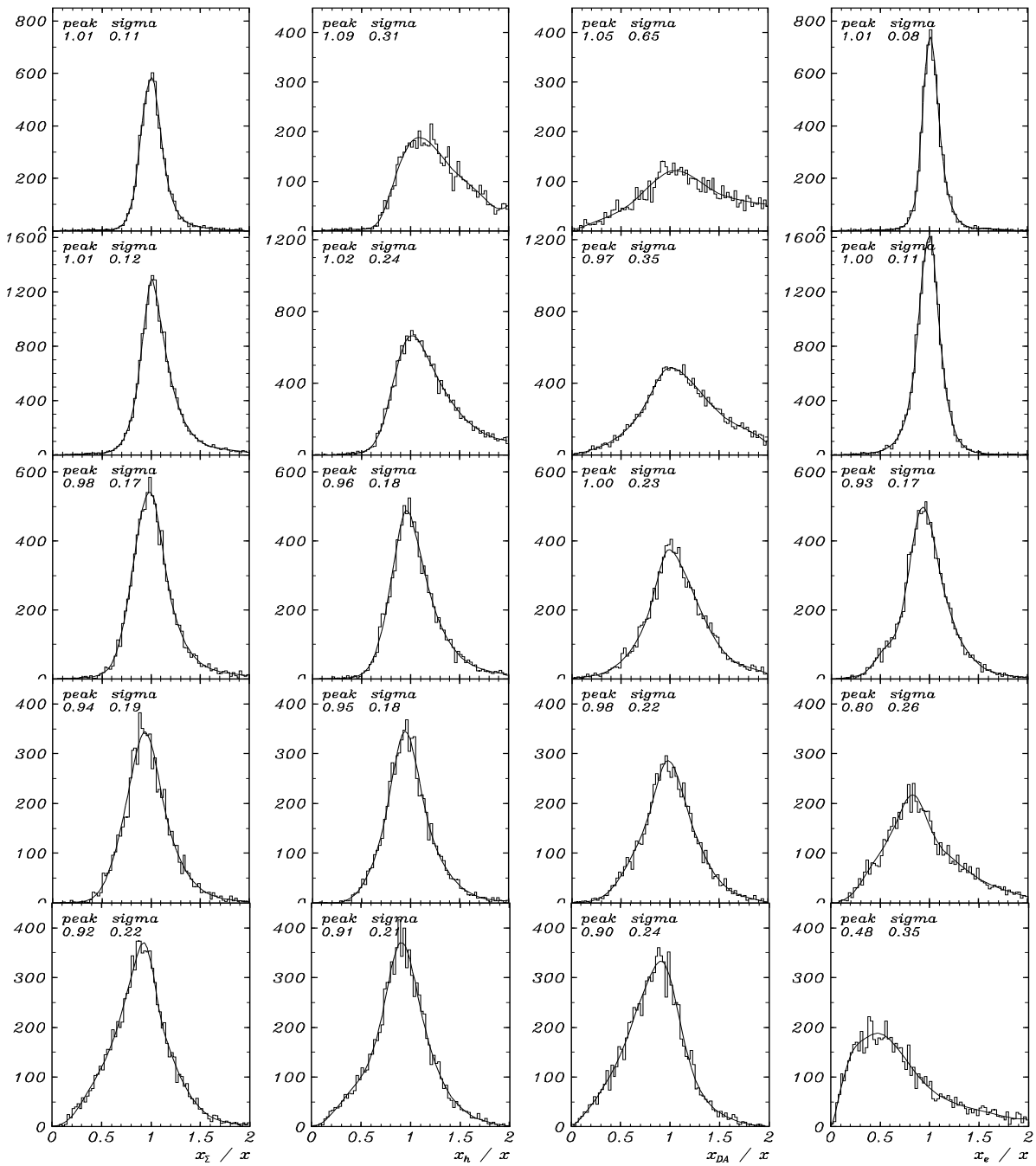

Figure 2: *Comparison x_{method}/x at low Q^2 ($Q^2 > 7\ GeV^2$) for the Σ, mixed , DA and e methods. From top to bottom, each row represent a bin in y: very high (0.5-0.8), high (0.2-0.5), medium (0.1-0.2), low (0.05-0.1), very low (0.01-0.05).*

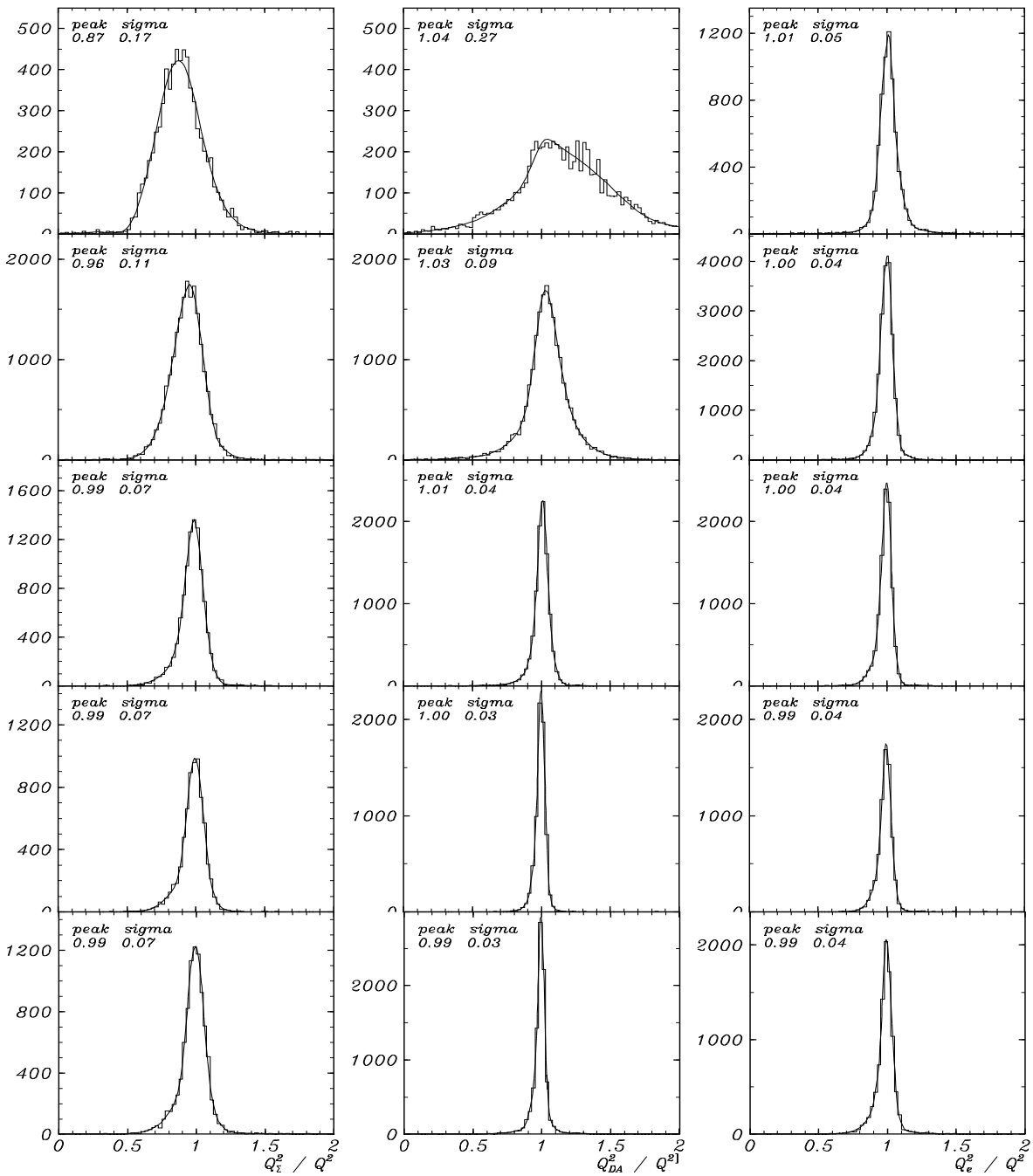

Figure 3: *Comparison Q^2_{method}/Q^2 at low Q^2 ($Q^2 > 7\ GeV^2$) for the Σ , DA and e methods. From top to bottom, each row represent a bin in y: very high (0.5-0.8), high (0.2-0.5), medium (0.1-0.2), low (0.05-0.1), very low (0.01-0.05).*

In conclusion, for the low x physics , i.e. at low Q^2, the Σ method allows to make a complete measurement in the full kinematic range. The e method remains the most precise method at high y, but now it can be compared to a hadronic method in the low x domain. The DA method is clearly disfavoured for low x physics at low Q^2. Finally the mixed method can be advantageously replaced by the Σ method.

4.2 Comparison at High Q^2

For this study, we request $Q^2 > 200\ GeV^2$ and the x_{method}/x distributions are shown in fig.4. The corresponding Q^2 distributions have all a gaussian shape, so we just give their mean value and standard deviation in table 1.

	Q^2_Σ/Q^2	Q^2_{DA}/Q^2	Q^2_e/Q^2
$0.5 < y < 0.8$	$0.89\ \sigma = 0.16$	$0.99\ \sigma = 0.07$	$0.99\ \sigma = 0.04$
$0.2 < y < 0.5$	$0.98\ \sigma = 0.08$	$0.99\ \sigma = 0.03$	$0.99\ \sigma = 0.03$
$0.1 < y < 0.2$	$1.01\ \sigma = 0.06$	$0.98\ \sigma = 0.03$	$1.00\ \sigma = 0.03$
$0.05 < y < 0.10$	$1.01\ \sigma = 0.05$	$0.98\ \sigma = 0.02$	$0.99\ \sigma = 0.03$
$0.01 < y < 0.05$	$1.02\ \sigma = 0.05$	$0.98\ \sigma = 0.02$	$1.01\ \sigma = 0.03$

Table 1: *Comparison Q^2_{method}/Q^2 at high Q^2 ($Q^2 > 200\ GeV^2$) for the Σ , DA and e methods.*

From fig.4 and tab.1 we can draw the following conclusions:

- The general behaviour of the Σ, the mixed and the e method have not changed, both in x and Q^2. A slight improvement in precision is visible at higher Q^2, which is clearly understood by a more precise energy measurement of the electron and of the hadrons.
- The DA method becomes more precise and improves at higher Q^2:
  - In x it has better resolutions than the Σ method for y between 0.05 and 0.3. It is more affected by losses in the beam pipe at very low y, and not as precise as the e or Σ methods at high y, but this last feature will disappear at very high Q^2 (above 2000 GeV^2).
  - In Q^2 it is very precise at medium and low y, and display a similar behaviour as Q^2_Σ at higher y, but without biases and better resolutions. The Q^2_{DA} resolution remains below 10% over the full y range.

In conclusion, it is also possible to make a very precise kinematics reconstruction at high Q^2, although this precision is not as important as at low Q^2 due to the fast decrease of the DIS cross-section with Q^2, which will always prevent at HERA a very fine "binning".

4.3 Effect of QED Radiation on Kinematic Reconstruction

In this section we study the QED radiation effect on the kinematic. We take the same selection criterias than in sect.4.1, but requesting now the presence of a radiated photon having an energy such that $1.5\ GeV < E^\gamma < 12.5\ GeV$, the upper bound coming from the Δ cut. The true x, y and Q^2 are defined at the hard interaction vertex taking into account

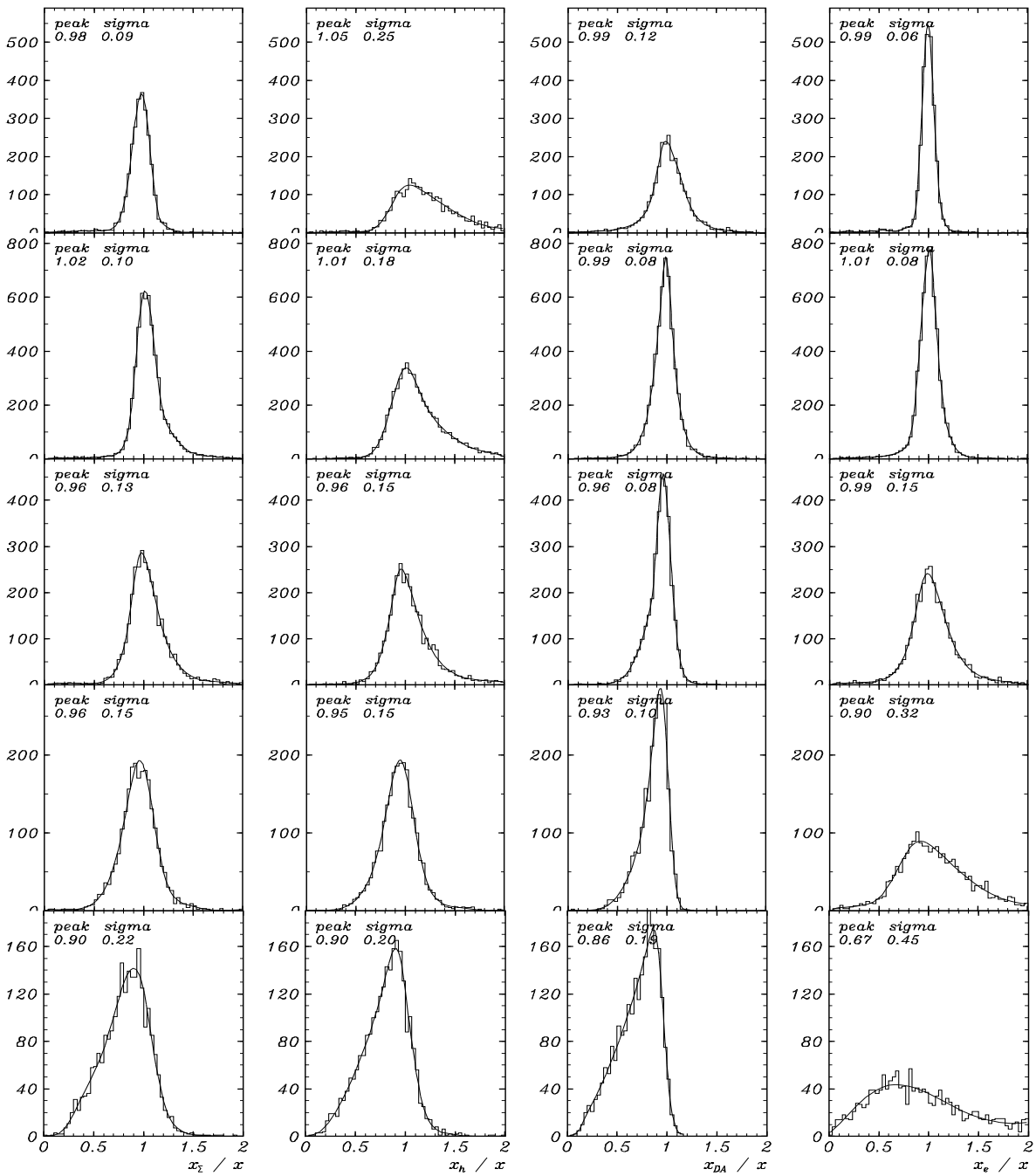

Figure 4: *Comparison x_{method}/x at high Q^2 ($Q^2 > 200\ GeV^2$) for the Σ, mixed , DA and e methods. From top to bottom, each row represent a bin in y: very high (0.5-0.8), high (0.2-0.5), medium (0.1-0.2), low (0.05-0.1), very low (0.01-0.05).*

the ISR or final state radiation (FSR) effects: For the ISR, these variables are computed assuming an incident electron energy equal to $E^e - E^\gamma$. For the FSR, the photon is summed with the electron. This is experimentally happening in most of the events since the colinear photon is merged in the cluster of energy deposited by the electron in the calorimeter.

Since the results are in general very similar to the ones obtained excluding the QED effects, we can just summarize this comparison on the biases and resolutions of the distributions with and without radiation.
i) the Q^2 reconstruction is essentially not affected by radiation in all the methods studied. The additional biases and enlargement of resolution are always smaller than 2%.
ii) the x reconstruction in the hadronic methods (m,DA,Σ) is also very stable against radiation, with changes of the order of 1 to 3%.
iii) the most affected variable is x_e when going at low y. The additional bias due to radiation on x_e/x is in the 5 bins, from very high to very low y: $-1\%, -5\%, -10\%, -20\%, -35\%$.

5 Beyond the Σ Method

5.1 The $e\Sigma$ Method

From the previous section, we can conclude that the Σ method can replace the mixed method and provide, with a single prescription, a precise F_2 measurement over the complete range covered by at least one the 4 basic methods [9]. It is however clear from figs.2-4 than the two most stable reconstruction for x and Q^2 all over the kinematic plane are x_Σ and Q^2_e. We can then simply define a so-called $e\Sigma$ method, in which the Q^2 is determined from the electron quantities, and x is reconstructed according to the Σ prescription:

$$x_{e\Sigma} = x_\Sigma \qquad Q^2_{e\Sigma} = Q^2_e \qquad y_{e\Sigma} = \frac{2\ E^e\ \Sigma}{(\Sigma + E(1-\cos\theta))^2} \tag{12}$$

The improvement brought by this method can also be observed on $y_{e\Sigma}$, by comparing its correlation $y_{e\Sigma}/y_e$ to the ones shown in fig.1, as can be also read in table 2. The correlation

	$0.2 < y < 0.5$	$0.5 < y < 0.5$
y_h/y_e	$0.88\ \sigma = 0.26$	$0.85\ \sigma = 0.27$
y_{DA}/y_e	$0.90\ \sigma = 0.22$	$0.96\ \sigma = 0.16$
y_Σ/y_e	$0.94\ \sigma = 0.17$	$0.97\ \sigma = 0.11$
$y_{e\Sigma}/y_e$	$1.00\ \sigma = 0.06$	$1.01\ \sigma = 0.03$
y_Σ/y	$0.95\ \sigma = 0.15$	$0.95\ \sigma = 0.11$
$y_{e\Sigma}/y$	$0.99\ \sigma = 0.09$	$0.99\ \sigma = 0.06$
y_e/y	$0.99\ \sigma = 0.06$	$0.99\ \sigma = 0.03$

Table 2: *Comparison of y reconstruction quality, for the Σ, mixed, DA, e and $e\Sigma$ method.*

with y_e is excellent at high y, in fact higher than its correlations to the generated y. We thus have a method which optimizes the reconstruction quality, but has the disadvantage of becoming correlated to the e method at high y and also to enlarge the small influence of radiative correction displayed by the Σ method as we shall see in section 6.

5.2 Kinematic Fitting

The ultimate improvement for the (x, Q^2) determination will come from a kinematical fitting procedure which use the full information in an optimal way. The weights on the redundant information coming from the electron and the hadronic final state have to be assigned depending on the kinematic of the event itself, and need, for a precise determination, a deep knowledge of the detector response. So far the fit has been performed using the conservation of Δ and of the transverse momentum [4, 19, 20] (for simplicity, we do not consider here the staightforward modification needed to treat the ISR case). This is equivalent to say that the fit has been performed using $[E, \theta, \Sigma, T]$ as measured variables and in fact using only $[E, \theta, \Sigma]$ since T is badly measured. It is then a posteriori clear why the fit behaves only slightly better than the e method at high y, the Σ method at medium y, and the Σ or m method at low y.

To go beyond this "3-variables fit" we need to include in the fitting procedure the information contained in the hadronic transverse momentum. This can be achieved by replacing (cf sect.2) T by the hadronic angle γ. We can then fit y and Q^2 according to the following equations

$$E(1-\cos\theta) = 2E^e(1-y) \qquad E\sin\theta = \sqrt{Q^2(1-y)} \tag{13}$$

$$\Sigma = 2E^e y \qquad \tan\frac{\gamma}{2} = 2E^e\sqrt{\frac{y^2}{Q^2(1-y)}} \tag{14}$$

hence the constraint equations can be written as

$$\Sigma + E(1-\cos\theta) = 2E^e \qquad \tan\frac{\gamma}{2} = \frac{2E^e - E(1-\cos\theta)}{E\sin\theta} \tag{15}$$

Assuming that the error covariance matrices has been determined for eqs.13-14, this fit will then provide everywhere a better result than any of the e, h, m, DA, Σ methods, i.e. it will also have the properties of the DA method like its high precision at large Q^2.

A complete study of the kinematic fitting is beyond the scope of this paper but we can conclude that there are at least two ways to become more precise than the basic or Σ methods, which both have the drawback that the measurement they can provide cannot be cross-checked a posteriori in a simple and independent way.

6 Comparison of QED Radiative Corrections

The size $\delta_{rc}(x, Q^2)$ of the QED radiative correction (r.c.) which has to be applied to the measured differential cross-section to obtain F_2 depends on the method used, since the cross-section is determined in bins of reconstructed x and Q^2. We have

$$\left(\frac{d^2\sigma}{dx\,dQ^2}\right)\left(\frac{1}{1+\delta_{rc}}\right) = \frac{2\pi\alpha^2}{xQ^4}(2-2y+\frac{y^2}{1+R})F_2(x,Q^2) \tag{16}$$

where $R \equiv \sigma_L/\sigma_T$ is the ratio of the cross-section of longitudinally and transversely polarised photons. The r.c. due to the virtual graphs, which are dominated by the fermion loops in the self-energy of the photon (vacuum polarization) can be included in a "running" $\alpha = \alpha(Q^2)$ in this equation [21]. These corrections are a function of Q^2 only, ranging from 5 to 13 %, for Q^2 between 5 and $10^4\ GeV^2$. The remaining δ_{rc} is dominated by the ISR from the lepton line

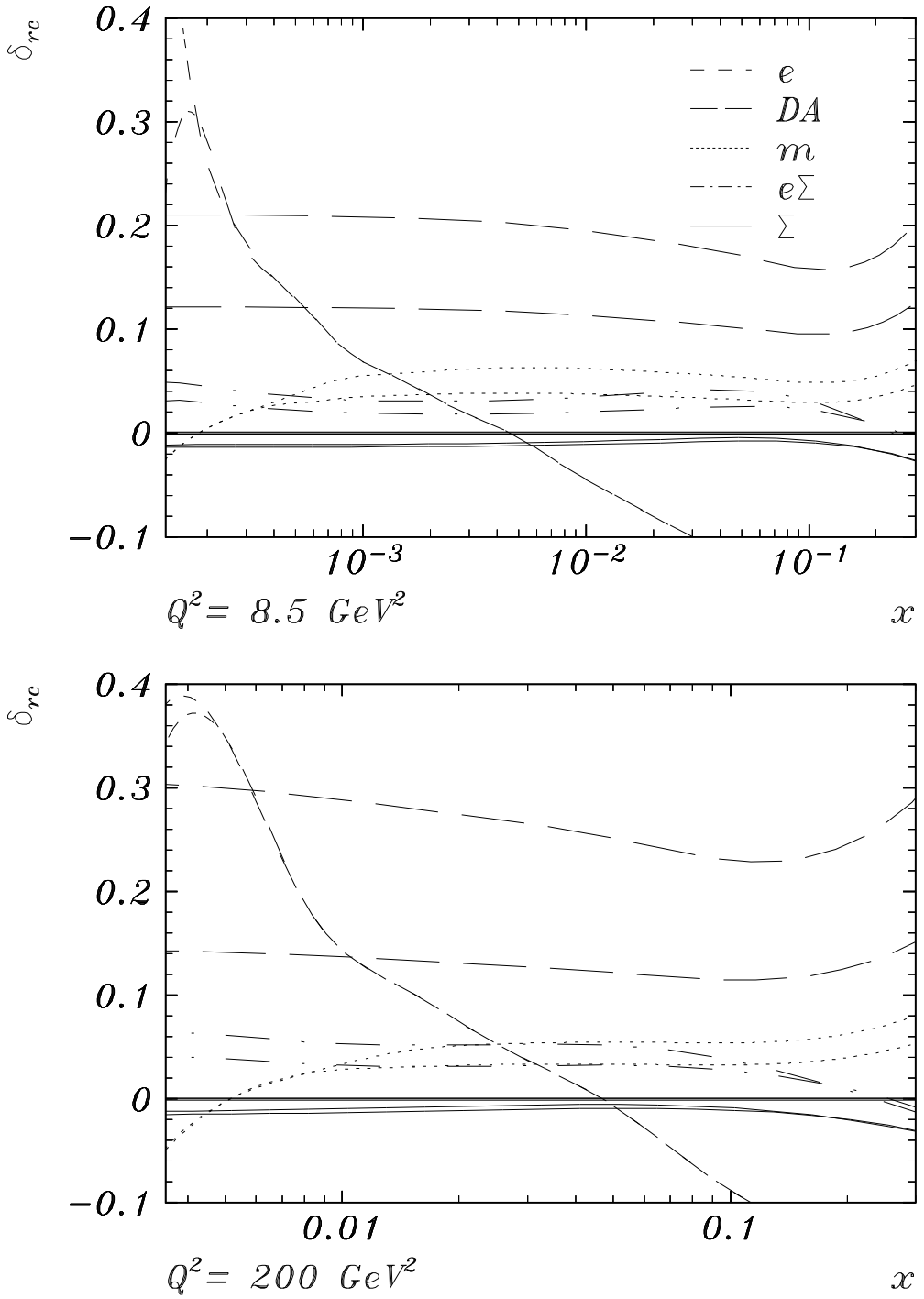

Figure 5: *Radiative corrections (excluding vacuum polarisation correction) as a function of x in two bins of Q^2 for the Σ, $e\Sigma$, DA, e and mixed method, requesting two minimal scattered electron energy: $E > 4\ GeV$ (upper curve of each method) and $E > 8\ GeV$ (lower curve).*

and is thus a sensitive probe to distinguish the r.c. behaviour for the different reconstruction methods.

The radiative corrections for the e, m,DA,Σ and $e\Sigma$ methods were obtained with the HELIOS program[22] in which they are calculated in the Leading Log Approximation up to $\mathcal{O}(\alpha^2)$, and cross-checked with the HERACLES program as implemented in DJANGO [10] for the e and Σ methods [23].

In fig.5 is shown as a function of x in 2 representative bins of Q^2 (8.5 and 200 GeV^2) the size of the radiative corrections for every method, without cut on Δ. We nevertheless take into account the minimal electron energy required for DIS identification. Two typical values have been used, $E = 4\ GeV$ and $E = 8\ GeV$, so two curves for each method are displayed. The variation of the r.c. for the 2 minimum energies can reach large values ($\delta_{rc}^{DA} \simeq 16\%$) for the DA or the e method, while it rather small for the m and $e\Sigma$ ($\delta_{rc}^{m,e\Sigma} \simeq 2\%$) and almost null for the Σ method. In the F_2 measurable region ($0.01 < y < 0.8$) there is no dependence on x or Q^2 neither for δ_{rc}^{Σ} nor, at the 2% level, for $\delta_{rc}^{e\Sigma}$, contrarily to δ_{rc}^{m} and δ_{rc}^{e} (dependence in x) or δ_{rc}^{DA} (dependence in Q^2). We can also remark that using the nominal s in the Σ method has a very small effect on the radiative corrections, since $\delta_{rc}^{\Sigma} \sim -1.5\%$.

The radiative corrections are therefore experimentally very difficult to control at the 1% level for the e and DA methods without introducing a cut on Δ of the events e.g. $\Delta > 30\ GeV$ which reduces the ISR effects. After such a cut all "hadronic" methods have r.c. displaying an almost constant behaviour in x and Q^2, and amounting at 8.5 GeV^2 to $\delta_{rc}^{tot} = \delta_{rc} + \delta_{rc}^{vac.pol.} \simeq$ +2, +5, +6, +9 % for the $\Sigma, e\Sigma, m$, DA methods respectively. There is still a dependence on x for δ_{rc}^{e}, which stops growing for y values above $z = \Delta/2E^e$.

We can conclude that the Σ method has small r.c. and that they barely depend on x, Q^2 or the presence of the Δ cut, therefore allowing to make a structure function measurement free of radiative corrections uncertainties. It is again complementary to the electron method which has r.c. varying as a function of x, and also dependent on the parton densities in the proton in the absence of a Δ cut.

7 DA and Σ Methods Independent of QED radiation

In case of initial state radiation of a photon from the electron we have $s_{true} = 4(E^e - E^\gamma)E^p$. To fully constrain the kinematics we need three independent variables and from the four variables defined in section 2, four combinations are possible. In practice only two [5] will deserve here our attention: the two which come directly from the DA and the Σ method.

The first of these methods was developped in [3], by determining the initial energy E^e from $[E, \theta, \gamma]$. Once E^e is reconstructed, it can be injected in the DA method to obtain the formulae for the double-angle method independent of ISR, labeled IDA here after:

$$E^e_{IDA} = E\ \frac{\tan\gamma/2 + \tan\theta/2}{\cot\theta/2 + \tan\theta/2} \qquad x_{IDA} = \frac{E}{E^p}\ \frac{\cot\gamma/2 + \cot\theta/2}{\cot\theta/2 + \tan\theta/2} \tag{17}$$

$$y_{IDA} = y_{DA} \qquad Q^2_{IDA} = E^2\ \tan\theta/2\ \frac{\tan\gamma/2 + \tan\theta/2}{\cot\theta/2 + \tan\theta/2} \tag{18}$$

[5] The other two methods uses 2 variables from the hadronic final state and only one from the electron, thus being less precise.

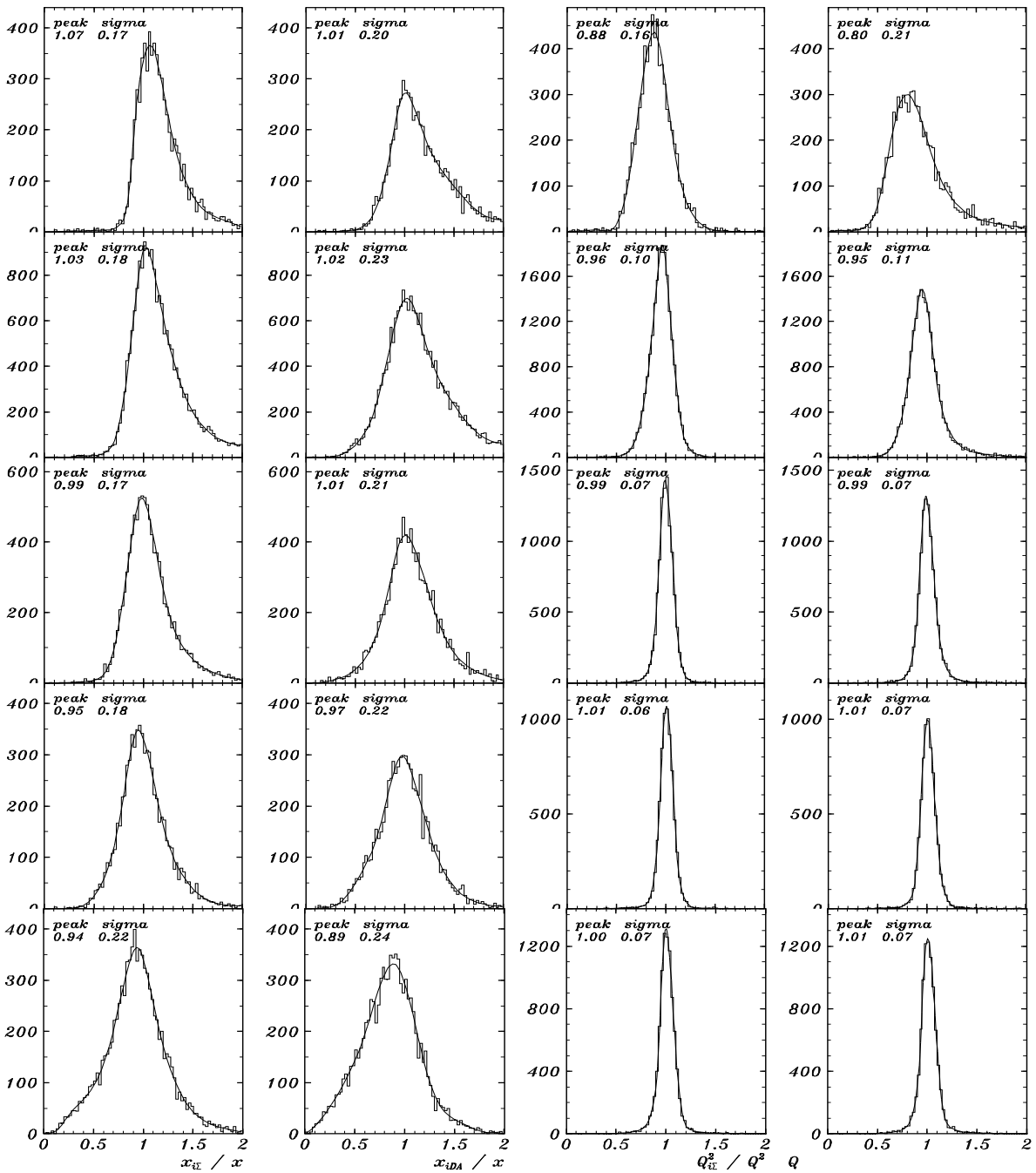

Figure 6: *Comparison of x and Q^2 reconstruction at low Q^2 ($Q^2 > 7\ GeV^2$) for Σ and DA method independent of initial QED-bremsstrahlung (IΣ,IDA) From top to bottom, each row represent a bin in y: very high (0.5-0.8), high (0.2-0.5), medium (0.1-0.2), low (0.05-0.1), very low (0.01-0.05).*

The other method is the Σ independent of ISR (IΣ), which is obtained by just using s_{true} instead of s [24]. We have $y_{I\Sigma} = y_\Sigma$, $Q^2_{I\Sigma} = Q^2_\Sigma$ and

$$E^e_{I\Sigma} = \frac{\Sigma + E(1-\cos\theta)}{2} \qquad\qquad x_{I\Sigma} = \frac{E}{E^p}\,\frac{\cos^2\theta/2}{y_\Sigma} \tag{19}$$

A comparison of the IΣ and IDA methods is presented in fig.6, following the scheme of figs.2-3. The following conclusions can be drawn.

- At low Q^2, the IΣ method is slightly more precise than the IDA one in all y bins both for x and for Q^2.
- $x_{I\Sigma}$ is less precise than x_Σ at high y, while they have similar resolutions at low and medium y.
- x_{IDA} and Q^2_{IDA} are more precise than their DA counterpart at low x, but have wider resolutions at low y.

The loss of precision when trying to reconstruct E^e is compensated by the reconstruction of the true kinematics when studying the special class of events with catastrophic initial state radiation. However for the structure function measurement it is better, as it has been done on the 1992 and 1993 data by the H1 and ZEUS collaborations [7, 9, 25, 26], to use the methods described in the preceding sections (e, m, DA, Σ) since the additional smearing observed in these two ISR independent methods is larger than the smearing introduced by QED radiation. These ISR independent methods can also be used as has been demonstrated by a complete F_2 analysis based on the IΣ method which has been done inside the H1 collaboration on the 1992 data [27], in good agreement with the published measurements.

8 Conclusion

We presented a new prescription for DIS kinematic reconstruction well adapted to study the low x-low Q^2 physics in the full y range $(0.01 < y < 0.8)$ and which allows to measure F_2 in the complete kinematic domain accessible at HERA. This Σ method can be modified to become fully independent of ISR (IΣ method) although this is not necessary, since the radiative corrections for the Σ were shown to be already very small, and some loss of precision when using the IΣ method was observed. By replacing Q^2_Σ by Q^2_e we defined another method which further optimizes the reconstruction precision at the cost of becoming correlated to the e method at high y. For the kinematic fitting we recommended to consider the hadronic angle instead of its transverse momentum as the second variable (beside Σ) characterizing the hadronic final state. After this review on the subject of reconstruction of the deep inelastic scattering kinematics at HERA, we expect that future improvements in this field will mostly come from deeper knowledge and better use of the detector response.

Acknowledgments

In this paper we relied extensively on the efforts of our H1 collaborators, with whom we built the software chain on which the quantitative results presented here are based upon, and we would like to thank them warmly. We also want to thank Johannes Blümlein for his interest in this work and for his great help on the radiative correction part. We finally would like to thank Joel Feltesse for usefull discussions and a careful reading of the manuscript.

Appendix: y, Q^2 and x formulae

method	y	Q^2	x
e	$1-\frac{E}{E^e}\sin^2\frac{\theta}{2}$	$4E^eE\cos^2\frac{\theta}{2}$	Q^2/ys
h	$\frac{\Sigma}{2E^e}$	$\frac{T^2}{1-y_h}$	Q^2/ys
m	y_h	Q_e^2	Q^2/ys
DA	$\frac{\tan\gamma/2}{\tan\gamma/2+\tan\theta/2}$	$4E^{e2}\frac{\cot\theta/2}{\tan\gamma/2+\tan\theta/2}$	Q^2/ys
Σ	$\frac{\Sigma}{\Sigma+E(1-\cos\theta)}$	$\frac{E^2\sin^2\theta}{1-y_\Sigma}$	Q^2/ys
IDA	y_{DA}	$E^2\ \tan\frac{\theta}{2}\frac{\tan\gamma/2+\tan\theta/2}{\cot\theta/2+\tan\theta/2}$	$\frac{E}{E^p}\frac{\cot\gamma/2+\cot\theta/2}{\cot\theta/2+\tan\theta/2}$
IΣ	y_Σ	Q_Σ^2	$\frac{E}{E^p}\ \frac{\cos^2\theta/2}{y_\Sigma}$

References

[1] J.Feltesse, "Physics at HERA", vol. 1, ed. R.D. Peccei, DESY (1987) 33-58

[2] A.Blondel, F.Jacquet, Proceedings of the Study of an *ep* Facility for Europe, ed. U.Amaldi, DESY 79/48 (1979) 391-394

[3] S.Bentvelsen et al., Proceedings of the Workshop Physics at HERA, vol. 1, eds. W. Buchmüller, G. Ingelman, DESY (1992) 23-40

[4] C. Hoeger, ibid., 43-55

[5] G.Bernardi, W.Hildesheim, ibid., 79-100

[6] J. Blümlein, M. Klein, Proceedings of the Snowmass Workshop "The Physics of the Next Decade", ed. R. Craven, (1990) 549-551

[7] H1 Collab., I. Abt et al., Nucl. Phys. B407 (1993) 515-535

[8] U.Bassler, Ph.D. thesis, University of Paris VI, May 1993.

[9] V. Brisson, LAL preprint 94-61 (1994), to appear in the proc. of the 27th International Conference on High Energy Physics, Glasgow (1994).

[10] G.A. Schuler, H. Spiesberger, Proceedings of the Workshop Physics at HERA, vol. 3, eds. W. Buchmüller, G. Ingelman, DESY (1992) 1419-1432

[11] A. Kwiatkowski, H. Spiesberger and H.-J. Möhring, ibid., 1294-1310

[12] L. Lönnblad, Computer Phys. Comm. 71 (1992) 15-31

[13] H1 Collab., T. Ahmed et al., Phys. Lett. B298 (1993) 469-478

[14] ZEUS Collab., M. Derrick et al., Z. Phys. C59 (1993) 231-242

[15] A.D. Martin, W.J. Stirling, R.G. Roberts, Proceedings of the Workshop on Quantum Field Theory Theoretical Aspects of High Energy Physics, eds. B. Geyer and E.M.Ilgenfritz (1993) 11-26

[16] R. Brun et al., GEANT3 User's Guide, CERN-DD/EE 84-1 (1987)

[17] H1 Collab., I. Abt et al., DESY 93-103 (1993) *submitted to Nucl. Instr. and Meth.*.

[18] U.Bassler, G.Bernardi, Kinematic Reconstruction inside H1, H1-note/LPNHE-Paris preprint, *in litt.*

[19] H. Chaves, R.J. Seyfert, G. Zech, Proceedings of the Workshop Physics at HERA, vol. 1, eds. W. Buchmüller, G. Ingelman, DESY (1992) 57-70

[20] J.P. Phillips, Manchester preprint MAN/HEP/93/9 (1993), H1-note 09/93-314 (1993)

[21] H. Spiesberger et al., Proceedings of the Workshop Physics at HERA, vol.2, eds. W. Buchmüller, G. Ingelman, DESY (1992) 798-838

[22] J. Blümlein, ibid., 1270-1284

J. Blümlein, DESY 94-044 (1994), Z. Phys. C (1994) *in press*

[23] U. Obrock, private comunication.

[24] U. Bassler, G. Bernardi, H1-note 09/93-274 (1993)

[25] ZEUS Collab., M. Derrick et al., Phys. Lett. B316 (1993) 412-426

[26] ZEUS Collab., M. Derrick et al., DESY 94-117 (1994) *submitted to Phys. Lett. B.*

[27] N.Wulff, Ph.D. thesis, University of Hamburg, (1994)